DESIGN AND DEVELOPMENT OF AN INFLATABLE SUPERSONIC TENSION CONE DECELERATOR

Ian G. Clark and Robert D. Braun

Guggenheim School of Aerospace Engineering, Georgia Tech, Atlanta, GA 30332
ian_clark@ae.gatech.edu

ABSTRACT

The current state of the art in planetary entry systems is rapidly reaching its limitations. Inflatable aerodynamic decelerators (IADs) represent a potential technology path that can relax the size and deployment limitations of aeroshells and parachutes. Historical programs aimed at developing IADs demonstrated favorable performance and structural behavior, yet for the most part were eventually discontinued. Two concepts in particular, the Attached Inflatable Decelerator and tension cone saw extensive theoretical development and testing. A summary of those efforts is presented as a historical basis for a current program to further mature the tension cone concept. That program includes both computational and wind tunnel evaluation of a deployable tension cone.

1. INTRODUCTION

Planetary entry systems have historically relied on aerodynamic drag for deceleration. However, the technology that generates this drag, namely rigid aeroshells and supersonic and subsonic parachutes, is quickly reaching its limitations. Supersonic parachutes in particular have been noted to provide decreasing drag and stability performance at Mach numbers above about 2.0. Inflatable aerodynamic decelerators (IADs) represent a potential technology path that can relax the size and deployment limitations of aeroshells and parachutes. That is, an IAD can serve to increase the drag area provided by a rigid aeroshell while still keeping the diameter of the aeroshell within launch vehicle payload fairing limits. Additionally, the aerodynamic characteristics of IADs allow them to be deployed at higher Mach numbers and dynamic pressures than can be achieved by current supersonic parachute technology. This combination of earlier deployment and increased drag over the rigid aeroshell allows for the landing of heavier payloads.

This paper reviews historical efforts aimed at developing supersonic IADs, in particular the Attached Inflatable Decelerator and tension cone concepts, and describes an analysis and test program designed to increase the technical maturity of an inflatable supersonic tension cone decelerator. For more comprehensive historical reviews on supersonic aerodynamic decelerators, the reader is directed to the survey paper of Cruz and Lingard [1]. Hypersonic inflatable decelerators are thoroughly reviewed in the survey papers of Rohrschneider and Braun [2] and Hall [3].

2. EARLY IAD DEVELOPMENT

The concept of an inflatable aerodynamic decelerator can be traced back to the early 1960's when NASA was beginning to develop robotic planetary exploration missions which would require atmospheric deceleration. During this time a variety of IAD configurations were explored with distinguishing characteristics that included the mounting approach (e.g. attached or trailing), inflation method (on-board inflation system versus ram-air), and shape (e.g. spherical or conical). Some of the first wind-tunnel experiments were performed by McShera [4] who explored drag and stability characteristics of five distinct trailing IAD designs at Mach numbers up to 4.65. These included two ram-air inflated configurations, shown in Figure 1, and three closed configurations requiring a separate inflation system, shown in Figure 2.

Of the five designs evaluated, McShera notes that all but the front inlet ram-air model were quite stable and lacked dynamic oscillations across a broad range of payload trailing distances. In the case of the front inlet configuration full inflation was never achieved and a mass-flow pulsation phenomena developed which subsequently led to vibratory fabric loading and eventual material failure. This behavior was eventually alleviated by the addition of a porous screen over the inlet and by adding cups to channel the flow into the IAD. Drag coefficients for all models varied between 0.6 and 1.1 with the ram-air models typically having lower drag coefficients.

Following McShera's initial wind tunnel investigations two primary shapes emerged that would garner a majority of subsequent IAD research efforts. The first of these was developed by Houtz [5] and centered around the concept of a so-called isotensoid IAD shape with fabric stresses that would be uniform in all directions. Beginning with

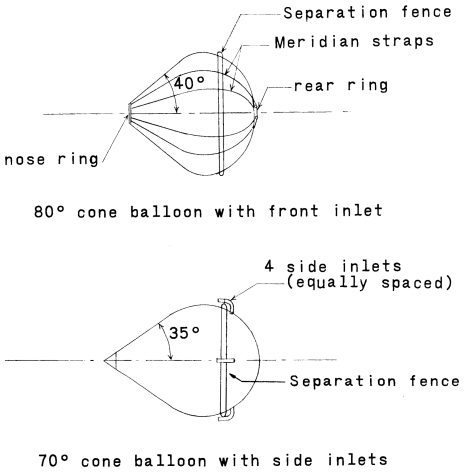

Figure 1. Early ram-air inflated aerodynamic decelerator configurations [4].

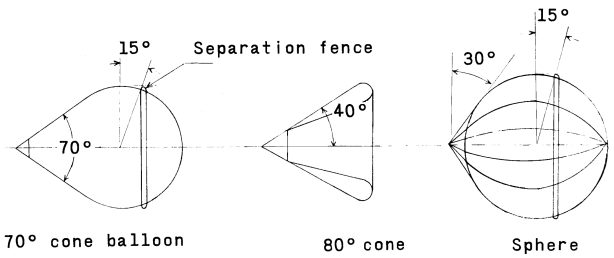

Figure 2. Early IAD configurations requiring a separate inflation system [4].

an input pressure distribution, Houtz was able to derive a set of differential equations which governed a family of shapes exhibiting constant fabric stress. Once an initial shape was derived, wind tunnel models could be fabricated and tested to attain an actual pressure distribution. This in turn could be passed back through Houtz's equations to arrive at a refined, iterated isotensoid shape. Additional iteration was possible, though typically not required. Examples of the type of shapes possible under this method are provided in Figure 3.

The isotensoid shape was evaluated as a trailing IAD in two separate atmospheric deployment tests with mixed results. Successful operation of a trailing four-foot diameter device with side mounted ram-air inlets was achieved at Mach numbers from 4.2 to 0.4 [7]. Drag coefficients for this test varied from 0.67 at Mach 4.2 to 1.45 at a Mach number of 1.25 and back down to roughly 0.9 in the subsonic regime. However, a later test of a similarly configured 18-foot diameter device failed to achieve inflation with the cause being attributed to severe whipping of the IAD and subsequent material failure of one of the ram-air inlets [8]. Though not discussed by the authors, this was possibly due to the separation distance from the payload being insufficient (the ratio of separation distance to payload diameter was approximately 4.7), thus causing the

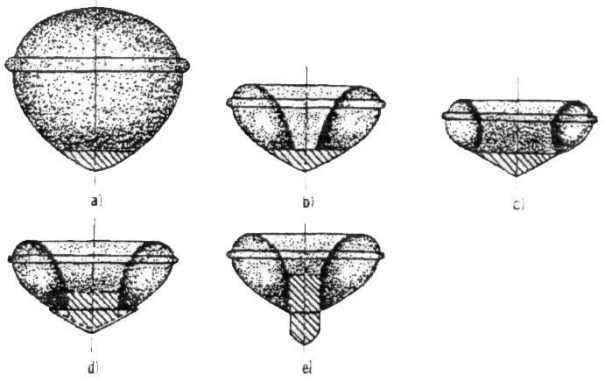

Figure 3. Example isotensoid IAD shapes [6].

IAD to be exposed to unfavorable wake.

Although tested as a trailing deceleration device, the isotensoid shape was predominantly evaluated as an attached IAD. In particular, concepts designed and fabricated by the Goodyear Corporation, who referred to them as attached inflatable decelerators (AIDs), saw extensive theoretical development and testing [9]. Typical design characteristics for these concepts are shown in Figure 4 and include a burble fence, gored construction, and coated fabric.

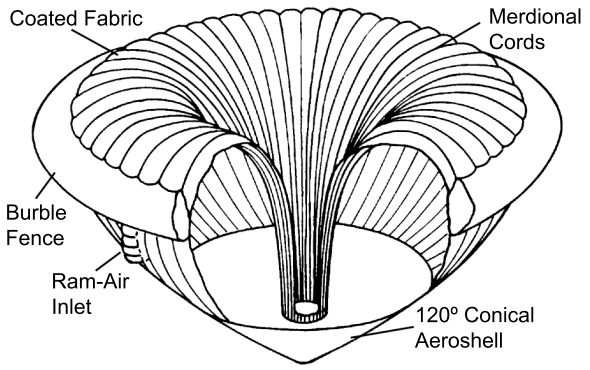

Figure 4. Design characteristics of the Goodyear AID concept (adapted from [6]).

The burble fence generally added another 5-10% to the maximum diameter of the AID model and served to provide constant point flow separation. Even though models incorporating the burble fence provided lower drag coefficients, the fence was nonetheless shown to be required for stability in the transonic and subsonic flight regimes [6]. The Nomex fabric was coated with Viton to reduce porosity.

The initial experimental program for the AID concept included a large-scale subsonic drop test, subsonic stability tests, and supersonic wind tunnel evaluation. The subsonic drop test was performed on a 36 ft. diameter model via helicopter at an altitude of 4800 ft. Despite experi-

encing high wind loads, the model successfully achieved ram-air inflation and produced a drag coefficient of 0.57 based on the total projected area. Stability tests included subjecting models to horizontal gust loads and observing the dynamic response. Results from these tests revealed that the AID configuration would align very quickly to the relative wind direction with little overshoot. The supersonic wind tunnel testing was performed on a 5 ft. diameter model, including a 5% burble fence, at Mach numbers of 2.2 and 3.0 and a dynamic pressure of 120 psf. Initial canopy deployment was assisted by an water-alcohol mixture that would vaporize at low pressure and thus provide the initial canopy pressurization, exposing the ram-air inlets to the free-stream. Test data showed excellent agreement with the theoretical methods used to predict performance and inflation behavior. A drag coefficient of 1.14 was reported at Mach 3.0, versus a modified Newtonian prediction of 1.16. The ratio of internal pressure to dynamic pressure was observed as 1.87, versus a predicted value of 2.0 based on isentropic flow relations. Additionally, the measured shape differed from the predicted in only the axial direction, where the measured depth value of 26.5 inches slightly exceeded the predicted depth of 24.85 inches. These results led the program to conclude that AID model performance was readily predictable. Other results of interest included full inflation times between 0.17 and 0.27 seconds, the insensitivity of the axial force coefficient to angle of attack variations of up to 5 degrees, and an overall lack of deployment "shock" loads commonly encountered during parachute inflation. This latter characteristic was likely due to the flow rate into the canopy decreasing as the internal pressure approached twice the dynamic pressure.

Ensuing wind tunnel tests on the AID configuration expanded the testing envelope to higher Mach numbers and lower dynamic pressures. Using the same 120° conical aeroshell and 5 foot diameter configuration as before, one test achieved successful deployment at a Mach number of 4.4 and dynamic pressure of 74.5 psf [10]. The test continued for a total of 66 minutes and included variations in dynamic pressure from 36 to 117 psf and angle of attack from 0 to 10 degrees. Steady and flutter free behavior was reported at all conditions tested.

Modifications to the basic 120° configuration shown in Figure 4 were also explored and included in several models fabricated by Goodyear [11]. Though they continued to employ canopy mounted ram-air inlets, later Goodyear models sought to eliminate the need for the water-alcohol solution by installing deployable inlets directly into the payload aeroshell, as shown in Figure 5. Another approach taken was to use a set of primary ram-air inlets located just behind the edge of the aeroshell forebody that would be deployed by springs. This set-up, shown in Figure 6, would eventually be tested on both a 120° and a 140° forebody. Results from tests using the 140° forebody yielded drag coefficients as high as 1.3 when the burble fence was removed but otherwise demonstrated similar performance to tests run using a 120° forebody [12]. These tests reinforced the notion that the AID's drag coefficient was relatively insensitive to variations in angle of attack, dynamic pressure, and Mach number.

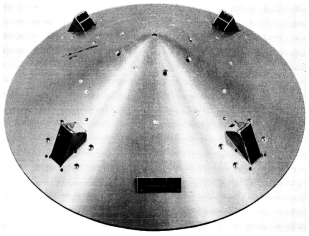

Figure 5. Deployable aeroshell ram-air inlets for AID inflation [11].

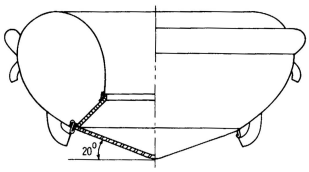

Figure 6. Spring loaded ram-air inlets on a 140° aeroshell (adapted from [12]).

Once initial results from the inflatable decelerator tests were reported, efforts were begun to analyze the flight regimes in which they would be favorable over traditional parachutes. For example, Anderson et al. recognized that the mass of a given decelerator was dependent on the loading, and thus dynamic pressure, at which it would be flown [13]. With that in mind, they developed mass estimating relationships for several different concepts as a function of size and loading conditions. These estimates were then scaled by each concept's drag area contribution, yielding a decelerator ballistic coefficient. Results from this analysis approach are shown in Figure 7, where the abscissa corresponds to a required drag area and dynamic pressure condition and the ordinate is the decelerator ballistic coefficient. In general, for a given dynamic pressure and drag area combination, a lower value of decelerator ballistic coefficient indicates a more efficient decelerator. Although the trailing isotensoid configuration performed poorly in Anderson's analysis, the attached AID configuration did show promise in cases that require large drag areas or were exposed to high dynamic pressures. These results highlight a key aspect of supersonic inflatable decelerators, that they perform well in supersonic environments but traditional parachutes tend to provide a more efficient solution in the subsonic regime.

Recognizing that parachutes are more efficient closer to terminal conditions, Bohon and Miserentino evaluated entry systems that utilized both an AID device and a terminal parachute [14]. Results comparing a combined parachute and AID system mass to landed payload mass for a Martian atmospheric entry are shown in Figure 8. Overall, Bohon and Miserentino concluded that inclusion of the supersonic AID allowed for deployment restrictions on the terminal parachute to be relaxed, leading to an increase in landed mass.

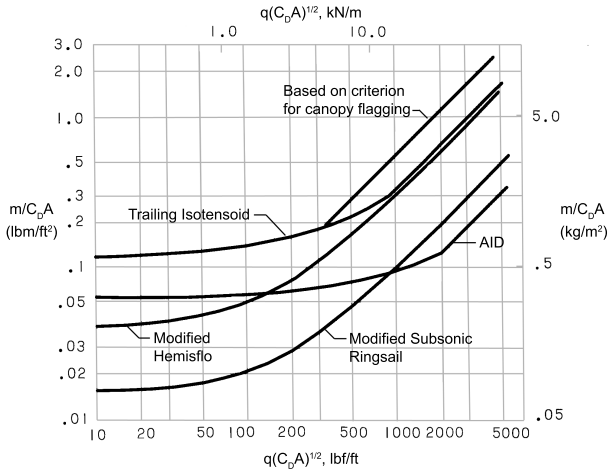

Figure 7. Decelerator ballistic coefficient as a function of a required drag area/dynamic pressure combination (adapted from [13]).

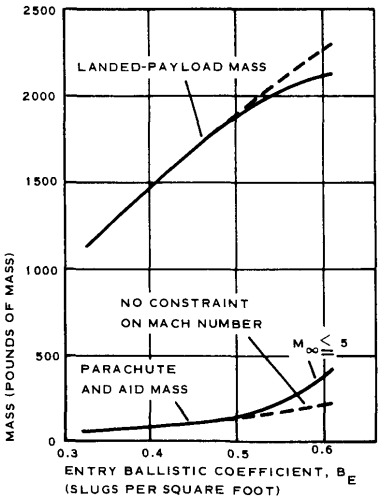

Figure 8. Combined AID/parachute masses and landed mass as a function of ballistic coefficient for a Mars entry (adapted from [14]). Solid lines correspond to entries constrained by heating limitations on the decelerator.

The significant research and development program surrounding the AID concept effectively ended in the mid 1970's. Though not discussed in program literature, the likely reason for this was the launch of the Viking probes to Mars and the subsequent absence of a mission requiring a supersonic decelerator. The AID concept was never incorporated into a planetary mission. However, it did find limited use as a stabilizer in munitions deployment programs managed by the US Air Force [15].

3. TENSION CONE DEVELOPMENT

Another configuration studied concurrently with the isotensoid shape was the tension cone. The tension cone concept, shown in Figure 9, consists of a flexible shell that is uniquely shaped so as to remain under tension and thus resist shape deformation. The shape itself is analytically derived on the basis of a predefined pressure distribution, a desired drag contribution of the tension shell, and an assumed constant ratio of circumferential to meridional stress. The tension in the shell is resisted at one end by a rigid forebody and at the other end by a compression ring, in some cases consisting of an inflated torus. Note that "tension cone" and "tension shell" are terms often used interchangeably in literature. However, in the context of this paper the tension cone corresponds to the entry device as a whole and tension shell refers to the axisymmetric portion between the rigid forebody and compression ring.

The initial theoretical development for the tension cone concept was done by Anderson et al. in 1965 [17]. Starting from linear membrane theory, Anderson derived a set of equations that could be used to solve for a unique tension shell shape from an initial axisymmetric pressure distribution. As with the AID concept, iteration on the

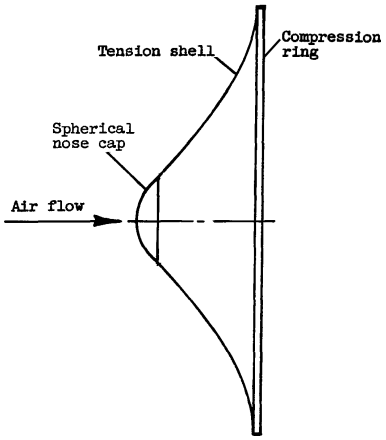

Figure 9. Typical tension cone decelerator [16].

shape was possible by first assuming a pressure distribution, testing that shape, and then passing the measured pressure distribution back through the analysis to arrive at a refined shape. In his initial work Anderson expanded the tension shell relations for cases assuming both Newtonian and uniform pressure distributions. It should be noted that although derivation of a tension shell shape requires an initial pressure distribution, the shape is in fact insensitive to changes in dynamic pressure. The relations also allow for one to solve for the circumferential and merdional stress resultants at any point along the shell, again assuming that the ratio of stress resultants is constant.

Some of the first experiments involving the tension cone focused on exploring the utility of the concept as a rigid aeroshell forebody. For example, buckling behavior of the tension shell was evaluated by Stroud and Zender

[18]. Using a variety of 35 cm diameter models fabricated from plastic sheets of varying thickness, Stroud and Zender attempted to simulate loading on the tension shell by putting a vacuum on the back side of the model and applying a vertical load on the nose. Three separate shapes were evaluated including a uniform pressure tension shell, Newtonian pressure tension shell, and a blunt cone shape. Both tension shell shapes were derived assuming a zero circumferential stress resultant. Results from their tests are shown in Figure 10.

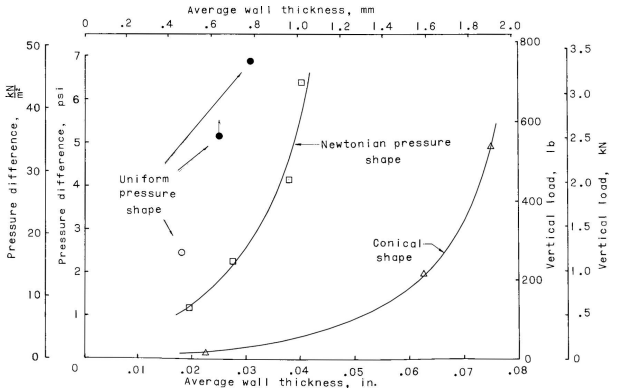

Figure 10. Buckling conditions for uniform and Newtonian tension shell shapes and blunt cone configurations [18]. Solid data points correspond to cases that did not buckle.

Based on these results, it was concluded that a Newtonian pressure derived tension shell would require roughly 50% more thickness than a uniform pressure derived tension shell. Both tension cone concepts showed significant advantages over the traditional blunt cone shape, with the blunt cone shape requiring wall thicknesses approximately 2.5 and 1.5 times that of the uniform and Newtonian shapes respectively. Stroud and Zender note that they could only simulate a uniform pressure loading and as a result the Newtonian tension shell experienced compression loads in the circumferential direction that otherwise would not have been present in an actual Newtonian pressure distribution. These compression loads likely led to the shape buckling earlier than would be generally predicted. Two of the three uniform pressure models failed to exhibit any buckling behavior and instead structural failure occurred when the tension shell separated from the nose cap.

Shortly after Anderson published his initial paper detailing tension shell theory several sets of wind tunnel tests were performed on small scale tension cone models with the goal of exploring aerodynamic and stability characteristics in supersonic and hypersonic condtions. The first of these evaluated nose bluntness and semi-vertex angle changes on multiple rigid models at Mach numbers of 3 [19] and 7 [20]. A defining characteristic of several configurations involved flow separation along the tension shell surface. In particular, models with shallow semi-vertex angles or blunt noses were susceptible to flow separation and double shock waves, as depicted in Figure 11.

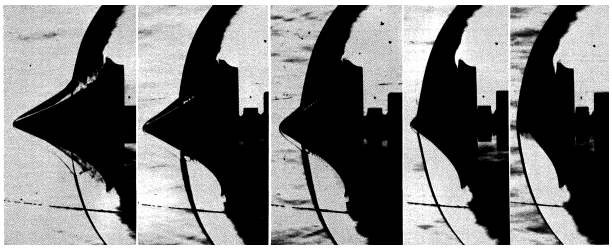

Figure 11. Schlieren imagery of tension shell shapes with a 5% diameter nose radius at Mach 3 and a 0° angle of attack [19]. Semi-vertex angles, from left to right, are 21.5°, 27.0°, 31.8°, 38.3°, and 47.0°.

Increases in angle of attack were also observed to trigger flow separation, with onset occurring later for models with larger semi-vertex angles. Of note is that the group of models with a semi-vertex angle of 47°, the largest evaluated, did not exhibit flow separation at nose radii up to 40% of the model's diameter or at angles of attack up to 12°. Reynolds number variations from 1-3 x 10^6 seemed to have little effect on the conditions of flow separation. Reported drag coefficients at Mach 3 varied from approximately 0.7 for the shallower vertex angle models up to 1.55 for the larger angle models. These values were consistently higher than those predicted by Newtonian theory, indicating that the Newtonian flow assumption used in deriving the tension shell shape was invalid. Static stability was achieved only on large vertex angle models and was roughly equivalent to that of a 60° cone.

Follow on wind tunnel tests performed in 1967 evaluated additional modifications to the tension cone geometry [21]. These predominantly consisted of varying the shoulder radius of curvature (the previous experiments had used a flat shoulder model) and shortening the diameter of the model by moving shoulder placement closer towards the nose of a given tension cone. This latter change is equivalent to reducing the flow turning angle since the shoulder is placed at a shallower point on the tension shell. The models were again run at Mach 3 and Reynolds numbers of 1 and 3 x 10^6. With regards to flow separation, models that rounded the shoulder and reduced the shoulder turning angle were more favorable, though, as shown in Figure 12, this generally came at the expense of drag coefficient. The shape modifications were observed to improve static stability. Calculations of the center of pressure location generally showed that a turning angle of no more than 70° was required to locate the center of pressure at the half-chord point.

As noted previously, drag coefficients that were being attained from wind tunnel experiments generally failed to match the Newtonian predicted drag coefficient, suggesting that the Newtonian flow approximation was a poor one. Examination of the tension cone shock structure indicates that the fundamental assumption in Newtonian flow, that the shock and body are almost coincident and the flow is moving nearly parallel to the surface, is not adhered to. The first analysis of the effect of this idiosyn-

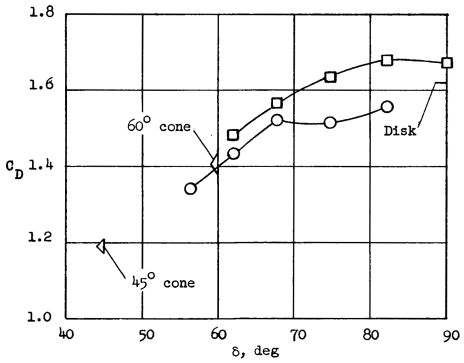

Figure 12. Drag coefficient variation versus shoulder flow turning angle, δ, for a pointed tension cone at Mach 3 and 0° angle of attack [21]. Squares and circles correspond to sharp and rounded shoulder radii, respectively.

crasy on the derived tension shell shape was performed by Sawyer in 1970 [16]. Sawyer generated two separate tension cone pressure models, one derived using a Newtonian flow assumption and the other using a pressure distribution derived from integral-relation theory (see [22]), with the latter lacking an analytical solution and thus requiring iteration on the derived tension cone shape. The final shapes along with the assumed and experimental pressure distributions are shown depicted in Figure 13.

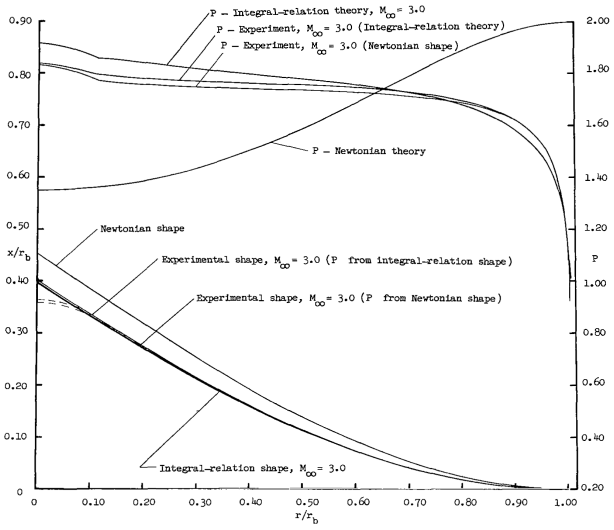

Figure 13. Comparison of integral-relation, Newtonian, and experimentally derived shapes and pressure distributions at Mach 3 and 0° angle of attack [16].

Even though the assumed pressure distributions for each shape were drastically different, the final shapes differed by less than 10% in the axial direction, implying a relative insensitivity of the tension cone shape to pressure distribution. Furthermore, the experimentally attained pressure distributions differed little and were quite close to the assumed integral-relation pressure distribution. To conclude his analysis Sawyer took the experimentally attained pressures for both models and passed them through the tension theory relations to arrive at two final tension cone shapes. These last profiles were nearly identical to each other and deviated from the original integral-relation shape by less than 1%.

A majority of the inceptive work done in analyzing the tension cone concept was applied to rigid models rather than deployable, flexible models. However, structural aspects of inflatable tension cones were not ignored and several important studies were undertaken. For example, Weeks recognized that inflatable rings could be advantageous as stiffening elements in deployable entry decelerators, such as a tension cone compression ring, and thus analyzed buckling behavior for a pressurized torus [23]. Assuming a membrane material that contributed zero bending stiffness to the torus wall, Weeks examined conditions leading to both an in-plane buckling mode and and out-of-plane, twisting mode. Loads leading to buckling were noted to be dependent on the manner in which they were applied during buckling, so criteria were developed for conditions of constant-direction loading, radial loading, and for the in-plane mode only, hydrostatic loading. Solutions for each of those criteria indicated that for identical geometries and material properties, out-of-plane buckling would occur for lower loading conditions than in-plane buckling. Within each mode, a condition of constant-direction loading was calculated to induce buckling at a lower load than for the condition of radial loading. Weeks also pointed out that it was advantageous to minimize the ratio of torus cross-sectional radius to total radius as it increased the critical buckling load.

Testing and validation of the relations developed by Weeks was performed as part of a larger study on tension cone deployment mechanics by Kyser [24]. In these tests tori of two different slenderness ratios were manufactured and placed in laboratory rigs capable of applying uniform compressive loads and simulating a radial loading condition. The testing rigs employed consisted of a toggle harness and a vacuum bag, depicted in Figure 14. Of note is that tori were manufactured by winding Dacron fiber over an elastomer bladder and then bonding the fiber to the bladder with resin. This required augmentation of Weeks' original buckling relations and a netting analysis was used to estimate the material section properties that resulted. In addition to the in-plane

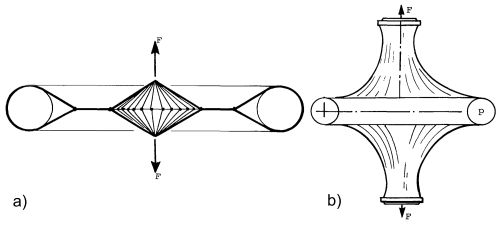

Figure 14. Toggle harness (a) and vacuum bag (b) instruments used for evaluating torus buckling (adapted from [24]).

and out-of-plane buckling modes, these tests also looked for a localized wrinkling mode of the torus walls which would occur when the compressive hoop force applied to the torus exceeded the hoop pre-tension associated with torus pressurization. Results from the vacuum bag tests on the slender torus are shown in Figure 15.

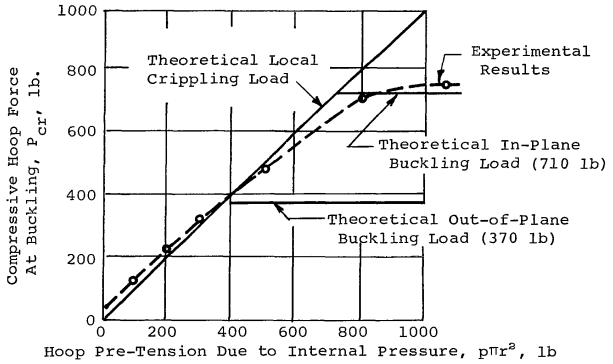

Figure 15. Buckling load results on a slender, filament-wound torus tested in a vacuum bag harness [24].

For the slender torus theoretical predictions of the conditions of localized wrinkling of the torus wall were shown to match very well with test data. In-plane buckling required slightly higher loads than predicted. Buckling was observed to occur very rapidly and shortly after the first appearance of localized wrinkling. Out-of-plane buckling failed to occur at all, an outcome attributed to the vacuum bag restricting motion to the only a radial direction. Testing on the more stout torus demonstrated similar agreement with theory, though with a small amount of conservatism. The stout torus was also used to evaluate the torus pressure at which the torus recovered from buckling. Required recovery pressures were consistently lower than predicted and tended to decrease as multiple failures and recoveries were performed, thus hinting at a "memory" characteristic of the structure. Results from the toggle harness were not reported as the test apparatus was determined to be too restrictive of both buckling mode behaviors.

Kyser's study of tension cones also entailed the development of a model to predict the required torus pressure needed for tension cone deployment [24]. In his model, Kyser assumed that deployment was dependent on the torus developing a "hinge moment" sufficient to recover from an initially folded orientation. Simulations of tension cone deployment were performed using an inflatable model deployed underwater at dynamic pressures up to 250 psf. Deployment behavior during these tests was observed to be better than predicted and the torus pressures required to fully deploy the tension shell were roughly 60% of that estimated from the derived model, as shown in Figure 16. Buckling modes induced at higher dynamic pressure were more benign than in the vacuum bag tests and tended to occur much more gradually. However, considerable elastic motion in the form of pitching and pumping of the inflated torus was observed and the

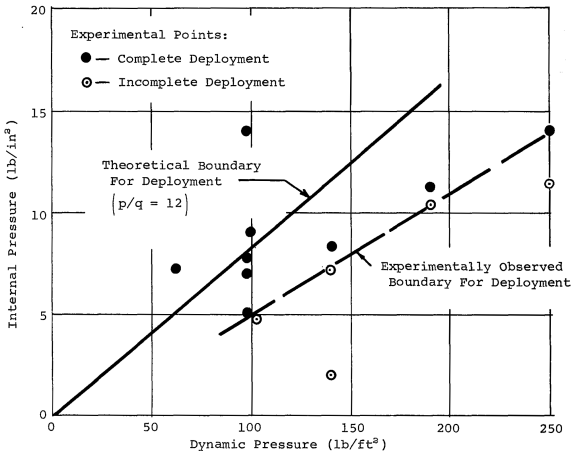

Figure 16. Results of underwater deployment tests of a tension cone [24].

tension cone model exhibited drag force oscillations with an amplitude of 10% and a frequency of 3-4 Hz. This behavior was attributed to the fabricated shape of the tension shell being poorly suited for low-subsonic flow. Severe surface wrinkling on the tension shell surface was noted and would indicate that circumferential loads beyond those assumed in the tension shell shape derivation were present.

4. CURRENT TENSION CONE DEVELOPMENT

The current efforts aimed at maturing the tension cone concept are primarily being pursued by The Program to Advance Inflatable Decelerators for Atmospheric Entry (PAI-DAE). Operated out of NASA's Langley Research Center, PAI-DAE has initiated several projects that will advance the state of the art of entry systems for the benefit of future robotic and human missions. Among these projects is the evaluation of a flexible tension cone. The development path being pursued by PAI-DAE for the tension cone IAD includes a series of wind tunnel tests that will provide data for the characterization of its performance and the validation of analyses. The first batch of testing will be conducted at the Unitary Plan Wind Tunnel at Langley Research Center and will consist of force and moment data gathering using a fully rigid tension cone model. The test objectives include the determination of the static aerodynamic coefficients, determination of the shock position and behavior, and a qualitative assessment of the stability of the flow field around the tension cone. The particular configuration being tested is shown in Figure 17. Key dimensions and parameters for this model are shown in Table 1. The planned entry date for this test is in mid-October of 2007. A follow on test of a similarly dimensioned rigid pressure model is currently planned for November of 2007. This model will include approximately 81 pressure ports located across the surface and backside of the model. These ports will

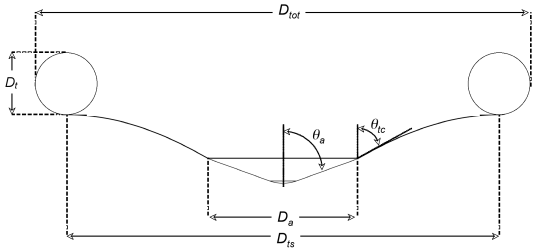

Figure 17. Rigid tension cone configuration.

Table 1. Rigid tension cone dimensions and parameters.

Quantity	Units	Value
Aeroshell Diameter, D_a	in.	1.8447
Tension Shell Diameter, D_{ts}	in.	5.25
Torus Diameter, D_t	in.	0.75
Total Diameter, D_{tot}	in.	6.0
Aeroshell Half Cone Angle, θ_a	deg.	70
Tension Cone Half Cone Angle, θ_{tc}	deg.	60

be used to ascertain the pressure distribution along the surface and backside of the tension cone model. A range of testing conditions for both sets of testing is included in Table 2.

The PAI-DAE program is also planning a second round of testing at the Glenn Research Center 10' x 10' Supersonic Wind Tunnel. This set of testing will include two separate model configurations, both of which will be 60 cm. diameter scaled versions of the Unitary models. The first configuration will consist of a flexible tension shell attached to a rigid torus. This model will allow for characterization of any aeroelastic phenomena that may exist for flexible tension cones. A second configuration will replace the rigid torus with a full flexible and inflatable torus. As opposed to the rigid torus configuration which begins testing in a pre-deployed state, this configuration will allow for examination of the inflation and deployment behaviors of a tension cone. This round of testing is currently scheduled for January of 2008.

Table 2. Testing conditions for rigid tension cone model at the Langley Unitary Tunnel.

Condition	Minimum	Maximum
Mach Number	1.5	4.5
Dynamic Pressure, psf.	228	506
Total Pressure, psf.	891	8267
Angle of Attack	-12°	20°
Angle of Sideslip	-12°	12°

ACKNOWLEDGMENTS

The authors would like to acknowledge Juan Cruz and Neal Cheatwood for their guidance and review of this paper.

REFERENCES

[1] Cruz, J. R. and Lingard, J. S., "Aerodynamic Decelerators for Planetary Exploration: Past, Present, and Future," AIAA Paper 2006-6792, August 2006.

[2] Rohrschneider, R. R. and Braun, R. D., "Survey of Ballute Technology for Aerocapture," *Journal of Spacecraft and Rockets*, Vol. 44, No. 1, January-February 2007, pp. 10–23.

[3] Hall, J. L., "A Review of Ballute Technology for Planetary Aerocapture," IAA-L-1112, 2000.

[4] Jr., J. T. M., "Aerodynamic Drag and Stability Characteristics of Towed Inflatable Declerators at Supersonic Speeds," NASA TN-D-1601, March 1963.

[5] Houtz, N., "Optimization of Inflatable Drag Devices by Isotensoid Design," AIAA Paper 64-437, July 1964.

[6] Jr., M. M. M. and Bohon, H. L., "Development Status of Attached Inflatable Declerators," *Journal of Spacecraft and Rockets*, Vol. 6, No. 6, June 1969, pp. 654–660.

[7] Usry, J., "Performance of a Towed 48-Inch-Diameter (121.92-cm) Ballute Decelerator Tested in Free Flight at Mach Numbers From 4.2 to 0.4," NASA TN-D-4943, February 1969.

[8] Mayhue, R. J. and Eckstrom, C. V., "Flight-Test Results From Supersonic Deployment of an 18-Foot-Diameter (5.49-Meter) Towed Ballute Decelerator," NASA TM-X-1773, May 1969.

[9] Barton, R. R., "Development of Attached Inflatable Decelerators for Supersonic Application," NASA CR-66613, May 1968.

[10] Bohon, H. L. and Miserentino, R., "Deployment and Performance Characteristics of 5-Foot Diameter (1.5 m) Attached Inflatable Decelerators From Mach Number 2.2 to 4.4," NASA TN-D-5840, August 1970.

[11] Faurote, G. L., "Design, Fabrication, and Static Testing of Attached Inflatable Decelerator (AID) Models," NASA CR-111831, March 1971.

[12] Bohon, H. L., Sawyer, J. W., and Miserentino, R., "Deployment and Performance Characterisitics of 1.5-Meter Supersonic Attached Inflatable Decelerators," NASA TN-D-7550, July 1974.

[13] Anderson, M. S. and Bohon, H. L., "A Structural Merit Function for Aerodynamic Declerators," NASA TN-D-5535, 1969.

[14] Bohon, H. L. and Miserentino, R., "Attached Inflatable Decelerator (AID) Performance Evaluation

and Mission-Application Study," *Journal of Spacecraft and Rockets*, Vol. 8, No. 9, September 1971, pp. 952–957.

[15] Flatau, A., Olson, D. N., and Miller, M. C., "The Use of an Attached Inflatable Declerator for Store Delivery From High Speed Aircraft From Low Altitude," AIAA Paper 70-1199, September 1970.

[16] Sawyer, J. W., "Effects of Pressure Distributions on Bluff Tension-Shell Shapes," NASA TN-D-5636, February 1970.

[17] Anderson, M. S., Robinson, J. C., Bush, H. G., and Fralich, R. W., "A Tension Shell Structure for Application to Entry Vehicles," NASA TN-D-2675, March 1965.

[18] Stroud, W. J. and Zender, G. W., "Experimental Investigation to Determine Utility of Tension Shell Concept," NASA TM-X-1211, March 1966.

[19] Deveikis, W. D. and Sawyer, J. W., "Aerodynamic Characteristics of Tension Shell Shapes at Mach 3.0," NASA TM-D-3633, 1966.

[20] Robinson, J. C. and Jordan, A. W., "Exploratory Experimental Aerodynamic Investigation of Tension Shell Shapes at Mach 7," NASA TN-D-2994, September 1965.

[21] Sawyer, J. W. and Deveikis, W. D., "Effects of Configuration Modifications on Aerodynamic Characteristics of Tension Shell Shapes at Mach 3.0," NASA TN-D-4080, August 1967.

[22] Jr., J. C. S., "Calculation of Axisymmetric Supersonic Flow Past Blunt Bodies with Sonic Corners, Including a Program Description and Listing," NASA TN-D-4563, May 1968.

[23] Weeks, G. E., "Buckling of a Pressurized Toroidal Ring Under Uniform External Loading," NASA TN-D-4124, August 1967.

[24] Kyser, A. C., "Deployment Mechanics For An Inflatable Tension-Cone Decelerator," NASA CR-929, November 1967.